Original Article

Preoperative peripheral blood lymphocyte subsets integrated with geriatric nutritional risk index for prognostic assessment in elderly colorectal carcinoma patients

Yuxin Wang, Yizhe Hao, Houjun Jia

Department of Gastrointestinal Surgery, The First Affiliated Hospital of Chongqing Medical University, Chongqing, China

Contributions: (I) Conception and design: Y Wang; (II) Administrative support: H Jia; (III) Provision of study materials or patients: None; (IV) Collection and assembly of data: Y Wang, Y Hao; (V) Data analysis and interpretation: Y Wang; (VI) Manuscript writing: All authors; (VII) Final approval of manuscript: All authors.

Correspondence to: Houjun Jia, PhD. Department of Gastrointestinal Surgery, The First Affiliated Hospital of Chongqing Medical University, No. 1 Friendship Road, Yuanjiagang, Yuzhong District, Chongqing 400042, China. Email: 13908329596@163.com.

Background: Prognosis in elderly colorectal cancer (CRC) patients is generally poor, predominantly attributable to the interrelated phenomena of immunosenescence and malnutrition. Current prognostic assessment tools typically evaluate nutritional and immune status in isolation, potentially overlooking the synergistic effects of these interconnected factors on patient outcomes. Therefore, this investigation aims to establish a comprehensive immuno-nutritional biomarker, integrating lymphocyte subset profiles and the Geriatric Nutritional Risk Index (GNRI), to prognosticate postoperative outcomes in elderly CRC patients.

Methods: A retrospective cohort of 201 elderly CRC patients undergoing curative resection at our institution between October 2018 and July 2020 was analyzed. Immunological and nutritional parameters were selected via least absolute shrinkage and selection operator (LASSO) regression to formulate a novel composite biomarker, designated as lymphocyte subsets-GNRI (LS-GNRI). Survival analyses employing Kaplan-Meier estimators and Cox proportional hazards models assessed the correlation of LS-GNRI with overall survival (OS) and disease-free survival (DFS). A prognostic nomogram integrating LS-GNRI and variables identified through multivariate Cox regression was constructed, with predictive accuracy and practicality evaluated via area under the curve (AUC), calibration plots (CAL), decision curve analysis (DCA), and clinical impact curves (CIC).

Results: Results indicated that the LS-GNRI biomarker demonstrated independent prognostic significance for elderly CRC patients [hazard ratio (HR): 0.323, 95% confidence interval (CI): 0.217–0.480, P<0.001]. Patients with elevated LS-GNRI exhibited significantly improved OS and DFS, with AUCs for 1-, 3-, and 5-year survival predictions of 0.763, 0.82, and 0.753, respectively. The nomogram incorporating LS-GNRI, age, carcinoembryonic antigen (CEA), tumor staging, *RAS* gene and *BRAF* gene exhibited high predictive performance (AUC: 0.872, 95% CI: 0.807–0.936) and demonstrated clinical utility.

Conclusions: In conclusion, LS-GNRI constitutes a robust composite biomarker for postoperative prognostication in elderly CRC patients. Furthermore, a prognostic nomogram incorporating LS-GNRI, patient age, CEA levels, tumor staging, *RAS* gene and *BRAF* gene enhances the accuracy of survival prognostication in elderly individuals diagnosed with CRC.

Keywords: Peripheral blood lymphocyte subsets; Geriatric Nutritional Risk Index (GNRI); colorectal cancer (CRC); elderly patients; prognosis

Submitted Aug 01, 2025. Accepted for publication Nov 25, 2025. Published online Jan 26, 2026.
doi: 10.21037/tcr-2025-1685
View this article at: https://dx.doi.org/10.21037/tcr-2025-1685

Introduction

Colorectal cancer (CRC) is the third most commonly diagnosed cancer worldwide and the second most frequent cause of cancer-related deaths (1). The majority of CRC cases occur in the elderly population, constituting over 50% of new diagnoses (2,3). Despite advancements in therapeutic strategies, including standardized curative resection and immunotherapeutic interventions, which have progressively enhanced patient survival rates, a considerable fraction of patients still suffer tumor recurrence and mortality (4). Consequently, the determination of valid prognostic biomarker is critical for optimizing risk assessment and clinical management in elderly CRC populations.

According to investigations by the World Health Organization and previous studies in geriatrics, individuals aged over 60 years exhibit a decline in immune function and nutritional status to varying degrees. The immunologic system plays a pivotal part in tumor suppression (5) and control of neoplastic development. However, immunosenescence significantly impairs immune competence in older adults, leading to diminished anti-tumor immune responses relative to younger individuals (6,7). Lymphocytes, as key effectors of cellular immunity, are intimately involved in tumor immunosurveillance and progression (8-10). Prior research has demonstrated that tumor-infiltrating lymphocytes are strongly tied to clinical outcomes (11), yet their assessment requires complex and costly histopathological techniques. Conversely, peripheral lymphocyte subsets—such as T lymphocytes and B lymphocytes—are more readily accessible and cost-effective for routine clinical evaluation. Evidence supports that peripheral blood lymphocyte phenotypes serve as reliable prognostic biomarkers across various malignancies and are closely linked to patient survival risk (12-14). Moreover, as a gastrointestinal neoplasm, CRC prognosis is significantly influenced by nutritional status. Malnutrition adversely affects therapeutic decision-making, increases complication rates, and elevates mortality risk (15,16). Geriatric populations demonstrate particular predisposition to undernourishment due to age-related declines in digestive absorption and metabolic function (17). The Geriatric Nutritional Risk Index (GNRI), has been constructed by Bouillanne *et al.* (18), provides an objective, straightforward prognostic tool relied on serum albumin concentration, current body weight, and ideal body weight, serving as an effective predictor of nutritional risk in elderly populations.

To date, there has been no comprehensive prognostic model for elderly CRC populations that integrates nutritional parameters and immune factors represented by lymphocyte subsets. At the same time, given the multifactorial etiology of tumor progression, reliance on a singular biomarker may be inadequate. Therefore, this study proposes a combined prognostic framework that incorporates immune and nutritional indicators to establish a more robust and holistic risk stratification model. We present this article in accordance with the TRIPOD reporting checklist (available at https://tcr.amegroups.com/article/view/10.21037/tcr-2025-1685/rc).

Highlight box

Key findings

- Our investigation has been constructed a comprehensive immuno-nutritional biomarker, the lymphocyte subsets-Geriatric Nutritional Risk Index (LS-GNRI), integrating lymphocyte subsets and the Geriatric Nutritional Risk Index (GNRI), to enhance prognostic accuracy in elderly colorectal cancer (CRC) patients post-curative resection. Subsequently, a prognostic nomogram was constructed based on LS-GNRI, demonstrated robust predictive accuracy and clinical utility.

What is known and what is new?

- Previous research has established that immunological profile and nutritional status are pivotal prognostic indicators in colorectal carcinoma patients. Nonetheless, there has been a lack of integrative analyses combining lymphocyte subset distributions with nutritional parameters for comprehensive prognostic modeling, particularly within geriatric CRC populations.
- We analyzed a geriatric CRC cohort and established a novel immuno-nutritional biomarker, LS-GNRI, demonstrated its role as an independent prognostic indicator.

What is the implication, and what should change now?

- We should prioritize the assessment of immunological and nutritional biomarkers in geriatric colorectal oncology patients to enable prompt nutritional intervention within optimal physiological parameters. Additionally, future investigations should explore the synergistic efficacy of integrated immunotherapeutic and nutritional modalities.

Methods

Study population

We recruited 201 elderly patients diagnosed with CRC who underwent curative oncologic resection at The First Affiliated Hospital of Chongqing Medical University between October 2018 and July 2020. All

surgical interventions were radical resections. Inclusion criteria encompassed: (I) histopathological confirmation of colorectal adenocarcinoma; (II) age ≥60 years; (III) receipt of curative surgical resection; (IV) peripheral blood lymphocyte profiling via flow cytometry within one week prior to surgery, accompanied by complete blood count and hepatic function assessments; (V) availability of comprehensive clinical and pathological datasets. Exclusion criteria comprised: (I) active or chronic infectious processes; (II) prior history of other neoplasms; (III) autoimmune diseases; (IV) hematologic disorders; (V) severe organ failure; (VI) CRC is staged as stage IV.

The study was conducted in accordance with the Declaration of Helsinki and its subsequent amendments. The study was approved by the ethics committee of The First Affiliated Hospital of Chongqing Medical University (No. 2025-488-01) and individual consent for this retrospective analysis was waived.

Postoperative complications

To examine the correlation between the novel prognostic biomarker lymphocyte subsets-GNRI (LS-GNRI) and postoperative complications, we collected data on Postoperative complications, encompassing intra-abdominal infections within one month post-surgery, surgical site infections, anastomotic dehiscence, chyle leaks, intra-abdominal hemorrhage, and bowel obstructions.

Data source

Perform data extraction from the hospital's certified electronic medical record (EMR) system, including baseline demographic characteristics and clinical pathological parameters: age, sex, height, weight, family history of tumors, smoking history, alcohol consumption, chronic pulmonary diseases, chronic cardiovascular and cerebrovascular diseases, diabetes mellitus history, Tumor, Node, Metastasis (TNM) staging, tumor location, postoperative complications, and others. Hematological data encompass complete blood count, liver function tests, carcinoembryonic antigen (CEA) levels, and peripheral blood lymphocyte subset counts. Overall survival (OS) is determined through a standardized telephone follow-up carried out in July 2025, measuring the interval from surgery to mortality from all causes or last follow-up. Disease-free survival (DFS) is described as the interval from the date of surgery to the occurrence of recurrence, metastasis, mortality from all causes, or the last follow-up.

Statistical analysis

Quantitative variables conforming to a normal distribution are expressed as mean ± standard deviation, with intergroup comparisons conducted using independent samples *t*-tests. Non-normally distributed quantitative data are summarized by medians or interquartile ranges, with pairwise comparisons performed via Mann-Whitney *U* tests and multiple group comparisons utilizing Kruskal-Wallis *H* tests. Categorical variables are described by frequencies and percentages, with intergroup differences assessed through Chi-squared tests; when expected frequency counts are less than five, Fisher's exact test is applied. Spearman's rank correlation analysis is employed to elucidate the associations between various peripheral blood lymphocyte subtypes and the GNRI, with the correlation matrix visualized via a heatmap. A least absolute shrinkage and selection operator (LASSO) penalized regression model evaluates eleven selected immunological and nutritional biomarkers, culminating in the derivation of a composite hematological index, LS-GNRI, integrating lymphocyte subpopulations and GNRI. The model's classification performance is quantified using receiver operating characteristic (ROC) curves and area under the curve (AUC) metrics. Univariate and multivariate Cox proportional hazards regression analyses identify independent prognostic factors for OS. Optimal cutoff thresholds for LS-GNRI are determined using X-tile software based on OS, facilitating patient stratification. Survival outcomes are analyzed via the Kaplan-Meier method, with survival curves compared using the log-rank test. The five parameters—age, CEA, *RAS* gene, *BRAF* gene and staging—selected through Cox regression analysis, were combined with the LS-GNRI to design a nomogram. The predictive effectiveness of the nomogram was assessed by means of ROC curves and the AUC metric. Internal validation is performed via bootstrap resampling with 1,000 iterations to assess model stability and calibration curves (CAL) are plotted to compare predicted versus observed outcomes. Decision curve analysis (DCA) assesses the clinical net positive benefit of the model, while clinical impact curves (CIC) optimize decision thresholds to balance sensitivity and specificity. All statistical analyses are performed with SPSS (version 27.0) and R software (version 4.5.1). The best cutoff points are established using X-tile software (Yale University, New Haven, Connecticut, USA). A P value less than 0.05 is consider as statistically

Table 1 Baseline characteristics

Characteristic	N (%)
Age	
<75 years	145 (72.1)
≥75 years	56 (27.9)
Gender	
Female	67 (33.3)
Male	134 (66.7)
BMI, kg/m^2	
Normal (18.5–23.9)	120 (59.7)
Overweight (>23.9)	57 (28.4)
Underweight (<18.5)	24 (11.9)
Family history	
Yes	6 (3.0)
No	195 (97.0)
Smoking	
Yes	80 (39.8)
No	121 (60.2)
Drinking	
Yes	60 (29.9)
No	141 (70.1)
Comorbidity	
Yes	93 (46.3)
No	108 (53.7)
Tumor location	
Left colon	158 (78.6)
Right colon	43 (21.4)
Tumor stage	
I	38 (18.9)
II	102 (50.7)
III	61 (30.4)
Tumor differentiation	
Poor	33 (16.4)
Moderate	152 (75.6)
Well	16 (8.0)
Preoperative perforation/obstruction	
Yes	17 (8.5)
No	184 (91.5)
Postoperative complications	
Yes	15 (7.5)
No	186 (92.5)

BMI, body mass index.

significant.

Results

Patients' characteristics

This study included a cohort of 201 elderly CRC individuals who underwent eradication surgery. The baseline characteristics table summarizes their baseline demographic and clinicopathological characteristics (*Table 1*). All study participants were senior adults aged 60 years or older, with 53% in the 60–69 years age cohort, 37% in the 70–79 years cohort, 9% aged over 80, and 1% over 90. The mean age was calculated at 70 years. The male demographic comprised 134 individuals (66.7%), whereas the female cohort included 67 individuals (33.3%). A total of 93 patients (46.3%) present with chronic cardiovascular or cerebrovascular pathologies, diabetes mellitus, or chronic pulmonary disorders. According to the TNM classification system (AJCC 9th Edition), there were 38 cases (18.9%) categorized as Stage I, 102 cases (50.7%) as stage II and 61 cases (30.4%) as stage III. A total of 15 patients (7.5%) experienced postoperative complications. During follow-up, 41 patients (20.4%) succumbed to disease, whereas 160 patients (79.6%) remained alive, with a median follow-up period of 71 months. The median DFS and OS were 66 and 67 months, respectively.

Establishment of the LS-GNRI scoring system

We performed Spearman rank correlation analyses between patients' lymphocyte subset counts and the GNRI. The heatmap (*Figure 1*) illustrates their correlations, with R-values representing correlation coefficients; R-values and the intensity of the color indicates the strength of the association. Significant correlations were identified among these immunological parameters, particularly between total lymphocyte counts and total T lymphocyte populations, as well as between total T lymphocytes and CD4$^+$ T lymphocytes, which demonstrated the strongest correlation.

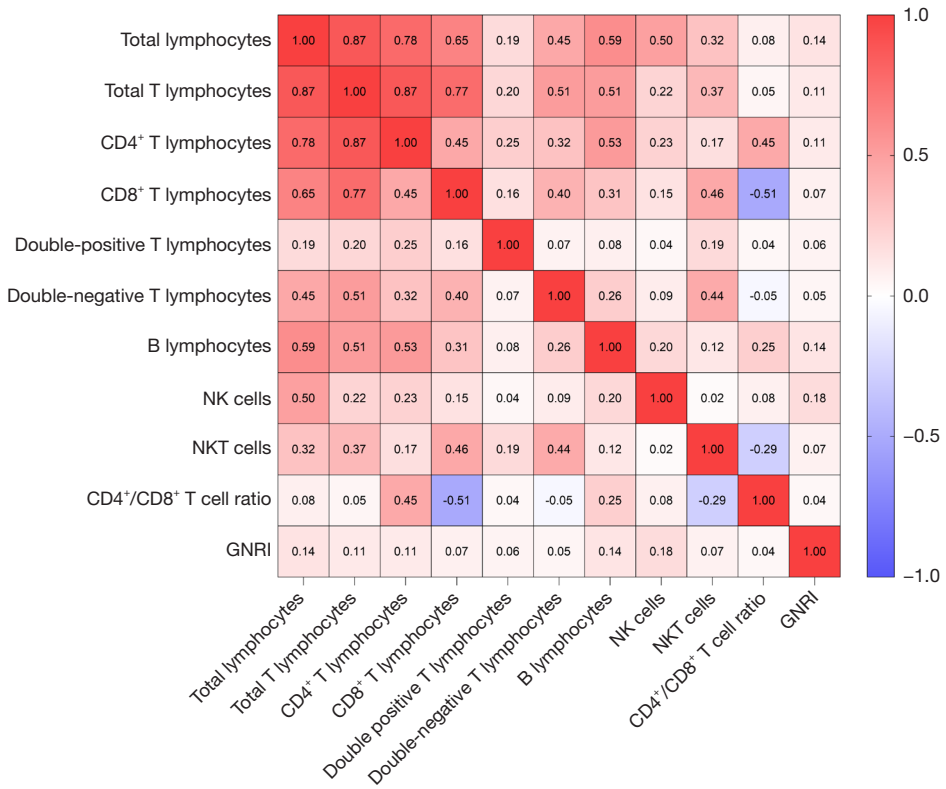

Figure 1 Heat map of the correlation between peripheral blood lymphocyte subsets and GNRI. The color depth and the size of the correlation coefficient indicate the strength of the association, with red or positive correlation coefficients signifying a positive correlation, and purple or negative correlation coefficients indicating an inverse relationship. GNRI, Geriatric Nutritional Risk Index.

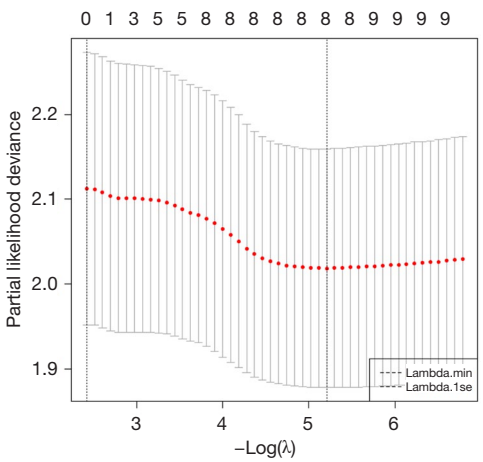

Figure 2 LASSO regression cross-validation for lymphocyte subset and GNRI selection. The vertical dashed lines denote the lambda.min (left) and lambda.1se (right) values. GNRI, Geriatric Nutritional Risk Index; LASSO, least absolute shrinkage and selection operator.

Given the high degree of multicollinearity among variables, the conventional Cox proportional hazards model was replaced with a LASSO penalized regression approach. Eleven immunological and nutritional biomarkers—total lymphocytes, total T lymphocytes, CD4$^+$ T cells, CD8$^+$ T cells, double-positive T cells, double-negative T cells, B lymphocytes, NK cells, NKT cells, the CD4$^+$/CD8$^+$ T cell ratio, and GNRI—were assessed for their prognostic relevance in CRC patients. The results are depicted via a LASSO cross-validation plot (*Figure 2*). To optimize model calibration and predictive accuracy, the lambda value corresponding to the minimum cross-validation error (λmin) was selected, leading to the identification of eight principal predictors—namely CD4$^+$ T cells, CD8$^+$ T cells, double-positive T cells, double-negative T cells, B cells, NK cells, the CD4$^+$/CD8$^+$ T cell ratio, and GNRI—for constructing a prognostic model of OS. The composite blood index derived is calculated as follows: LS-GNRI = (0.003 × CD4$^+$ T cells) – (0.005 × CD8$^+$ T cells) + (0.032 × double-positive T cells) + (0.001 × double-negative T cells) + (0.003 × B

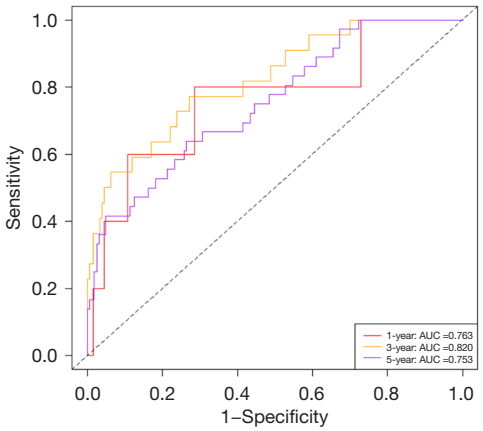

Figure 3 ROC curves of LS-GNRI for predicting postoperative survival at 1, 3 and 5 years. AUC, area under the curve; LS-GNRI, lymphocyte subsets-Geriatric Nutritional Risk Index; ROC, receiver operating characteristic.

cells) + (0.001 × NK cells) – (0.839 × $CD4^+/CD8^+$ T cell ratio) + (0.038 × GNRI). Subsequently, ROC curves for 1-, 3-, and 5-year postoperative OS were created based on LS-GNRI, with corresponding AUC values of 0.763, 0.82, and 0.753 (*Figure 3*).

Univariate and multivariate Cox proportional hazards regression analysis

Both univariate and multivariate Cox proportional hazards models demonstrated that high LS-GNRI functions as an independent protective factor for OS, with hazard ratio (HR) of 0.323 [95% confidence interval (CI): 0.217–0.480, P<0.001] and 0.533 (95% CI: 0.341–0.832, P=0.006), respectively. Furthermore, univariate Cox regression identified age, body mass index (BMI), tumor stage, CEA, alpha-fetoprotein (AFP), carbohydrate antigen 19-9 (CA19-9), *RAS* gene, *BRAF* gene and adjuvant chemotherapy as significant independent prognostic factors for OS (all P<0.05). Multivariate analysis corroborated that age (HR: 1.055, 95% CI: 1.008–1.105, P=0.02), advanced tumor stage (III versus I, HR: 15.419, 95% CI: 1.958–121.425, P<0.009), elevated CEA levels (HR: 1.021, 95% CI: 1.009–1.032, P<0.001), *RAS* gene mutation (HR: 2.586, 95% CI: 1.110–6.026, P=0.03) and *BRAF* gene mutation (HR: 8.115, 95% CI: 3.192–20.630, P<0.001) are independent predictors of OS (*Table 2*). Furthermore, acknowledging potential heterogeneity in immunonutritional status between geriatric patients aged over 75 and those aged 60–74 years, the study population was stratified into two age-based cohorts: the younger elderly (60–74 years) and the very elderly (≥75 years). Univariate and Multivariate Cox proportional hazards regression analyses within each subgroup demonstrated that the LS-GNRI served as an independent prognostic indicator in both groups, with statistically significant P values (less than 0.05).

Kaplan-Meier survival analysis

Using the optimal cutoff thresholds for LS-GNRI, as determined by X-Tile software, 201 individuals were stratified into three prognostic groups: high LS-GNRI high LS-GNRI (≥2.97), mid LS-GNRI (>2.39 and <2.97), and low LS-GNRI (≤2.39). Kaplan-Meier survival analysis demonstrated that elevated LS-GNRI levels were significantly associated with improved OS (P<0.001) compared to lower levels (*Figure 4A*). Similarly, higher LS-GNRI correlated with markedly enhanced DFS (P<0.001) (*Figure 4B*). In the figure, "N" denotes the number of cases in the cohort, and "n" represents the count of positive events within the group.

Subgroup analysis of LS-GNRI

To clarify the association between LS-GNRI and clinicopathological parameters in CRC patients, we conducted a comparative analysis across three stratified cohorts—high LS-GNRI, mid LS-GNRI, and low LS-GNRI—focusing on tumor localization, postoperative complications, preoperative perforation and obstruction, CEA serum levels, histological differentiation, tumor staging, *RAS* gene, *BRAF* gene, MSI and adjuvant chemotherapy, as detailed in the LS-GNRI subgroup analysis table (*Table 3*). The findings demonstrate that the low LS-GNRI cohort has a significantly higher prevalence of right-sided colonic neoplasms, elevated CEA levels, poorer histological differentiation, more *BRAF* mutation rates and more people undergoing adjuvant chemotherapy (All P values were less than 0.05). No meaningful statistical differences were detected in preoperative perforation or obstruction rates, postoperative complication rates, tumor staging, *RAS* gene mutation rates and MSI across the LS-GNRI stratifications.

Development and evaluation of nomogram

We has been constructed a prognostic nomogram for

Table 2 Univariate and multivariate analysis for overall survival

Variables	Univariate analysis		Multivariate analysis	
	HR (95% CI)	P	HR (95% CI)	P
Age	1.079 (1.055–1.140)	<0.001	1.055 (1.008–1.105)	0.02
Gender (male *vs.* female)	0.689 (0.370–1.283)	0.24	0.993 (0.400–2.465)	0.99
BMI	0.847 (0.763–0.941)	0.002	0.963 (0.867–1.070)	0.49
Family history (yes *vs.* no)	0.727 (0.100–5.288)	0.75	1.008 (0.089–11.463)	>0.99
Smoking status (yes *vs.* no)	0.757 (0.397–1.443)	0.40	1.795 (0.556–5.796)	0.33
Drinking status (yes *vs.* no)	0.603 (0.288–1.264)	0.18	0.519 (0.159–1.700)	0.28
Comorbidity (yes *vs.* no)	1.361 (0.737–2.516)	0.33	1.640 (0.767–3.507)	0.20
Tumor location (right colon *vs.* left colon and rectum)	1.429 (0.716–2.852)	0.31	0.631 (0.239–1.665)	0.35
Tumor stage				
Stage III *vs.* stage I	10.318 (2.441–43.615)	0.002	15.419 (1.958–121.425)	0.009
Stage II *vs.* stage I	2.725 (0.619–11.993)	0.19	1.932 (0.313–11.916)	0.48
Tumor differentiation				
Moderate *vs.* poor	0.559 (0.273–1.144)	0.11	0.449 (0.179–1.122)	0.09
Well *vs.* poor	0.164 (0.021–1.279)	0.08	0.295 (0.032–2.747)	0.29
Preoperative perforation/obstruction (yes *vs.* no)	2.233 (0.938–5.314)	0.07	0.847 (0.238–3.013)	0.80
Postoperative complications (yes *vs.* no)	0.623 (0.150–2.578)	0.51	0.943 (0.127–6.994)	0.95
CEA	1.015 (1.009–1.021)	<0.001	1.021 (1.009–1.032)	<0.001
AFP	1.097 (0.926–1.300)	0.28	1.083 (0.884–1.327)	0.44
CA19-9	1.010 (1.005–1.015)	<0.001	0.997 (0.989–1.006)	0.52
LS-GNRI	0.323 (0.217–0.480)	<0.001	0.533 (0.341–0.832)	0.006
RAS (mutant *vs.* wild-type)	2.616 (1.396–4.903)	0.003	2.586 (1.110–6.026)	0.03
BRAF (mutant *vs.* wild-type)	3.782 (1.956–7.312)	<0.001	8.115 (3.192–20.630)	<0.001
MSI (MSI-H *vs.* MSS)	0.797 (0.193–3.303)	0.76	0.260 (0.033–2.061)	0.20
Adjuvant chemotherapy (yes *vs.* no)	3.106 (1.377–7.010)	0.006	0.529 (0.132–2.115)	0.37

AFP, alpha-fetoprotein; BMI, body mass index; CA19-9, carbohydrate antigen 19-9; CEA, carcinoembryonic antigen; CI, confidence interval; HR, hazard ratio; LS-GNRI, lymphocyte subset-Geriatric Nutritional Risk Index; MSI, microsatellite-instability; MSI-H, microsatellite-instability high; MSS, microsatellite stable.

geriatric CRC patients by integrating the LS-GNRI index with independent prognostic markers identified via multivariate Cox proportional hazards regression analysis—patient age, tumor staging, *RAS* gene, *BRAF* gene and CEA serum levels (*Figure 5*). The ROC curve analysis demonstrated that the prognostic nomogram incorporating LS-GNRI achieved an AUC of 0.872 (95% CI: 0.807–0.936). In contrast, the conventional TNM staging system yielded an AUC of 0.717 (95% CI: 0.638–0.797), while the single GNRI indicator showed an AUC of 0.646 (95% CI: 0.557–0.735) (*Figure 6*). These findings suggest that the has been constructed nomogram offers enhanced predictive accuracy relative to both the traditional TNM classification or single nutritional assessment markers. Internal validation via bootstrap resampling (n=1,000) produces calibration plots indicating good model calibration (*Figure 7*). DCA confirms the model's clinical utility and net benefit (*Figure 8*). CIC demonstrate that at a risk threshold of 0.8, the predicted

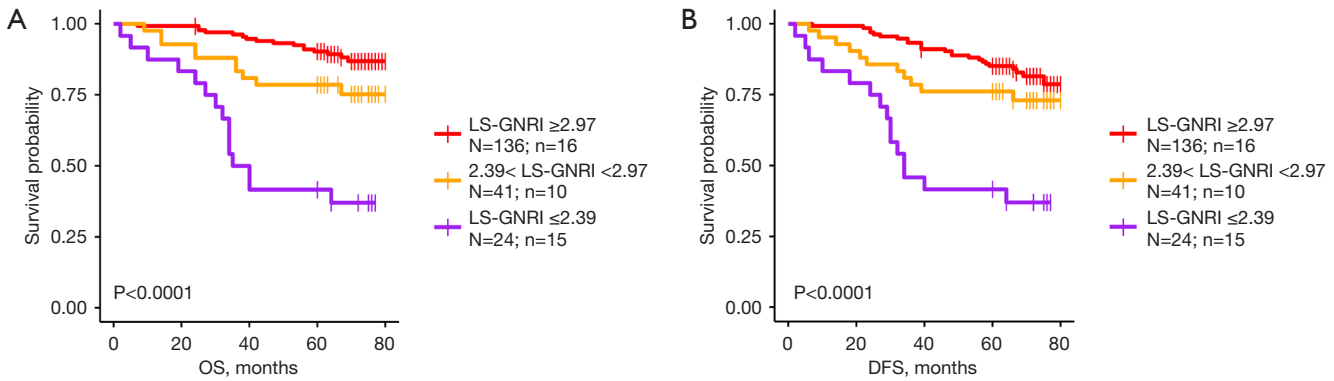

Figure 4 Survival analysis curve of LS-GNRI. Kaplan-Meier curves for (A) OS and (B) DFS. DFS, disease-free survival; LS-GNRI, lymphocyte subset-Geriatric Nutritional Risk Index; OS, overall survival.

quantity of high-risk patients closely corresponds to the observed quantity of adverse events (*Figure 9*).

Discussion

In our research, employing LASSO regression analysis, we constructed a prognostic biomarker, LS-GNRI, integrating peripheral blood lymphocyte subpopulations and GNRI. The results establish LS-GNRI as an independent prognostic indicator, with elevated scores tied to improved OS and DFS metrics. LS-GNRI exhibits significant associations with tumor localization, CEA levels, histological tumor differentiation, *BRAF* gene and adjuvant chemotherapy. A nomogram incorporating LS-GNRI, patient age, tumor staging, CEA levels, *RAS* gene and *BRAF* gene exhibits high predictive accuracy and substantial clinical utility for decision-making in this patient cohort.

Extensive prior research has demonstrated that immune competence is a pivotal determinant in the modulation of oncogenesis and tumor progression. Lymphocyte subsets, as key mediators of the host immune response, have attracted substantial scholarly focus. Simultaneously, nutritional status, serving as a prognostic biomarker, exerts a particularly influential impact on gastrointestinal malignancies, notably CRC. Yuan and colleagues conducted a retrospective analysis on a cohort of 86 CRC individuals who underwent standardized laparoscopic radical resection. They analyzed peripheral blood levels of $CD4^+$ and $CD8^+$ T cell, as well as the $CD4^+/CD8^+$ T cell ratio. Their results demonstrated that lymphopenia of $CD4^+$ T cells and a decreased $CD4^+/CD8^+$ ratio correlated with tumor progression and enhanced proliferative activity. Conversely, increased circulating $CD8^+$ T cell levels were tied to adverse clinical prognoses (19). Gao *et al.* reported that in a cohort of 171 gastric adenocarcinoma patients treated with curative gastrectomy, diminished peripheral T and B cell counts, coupled with an increased proportion of regulatory T cells (Tregs), served as independent prognostic biomarkers predictive of reduced relapse-free survival (RFS) (20). In 2019, Mao *et al.* analyzed the interrelation between circulating lymphocyte subsets and clinical prognosis in prostate adenocarcinoma patients, revealing that lower absolute counts of NK cells and $CD4^+$ T cells were significantly corresponds to poorer survival outcomes (21). Additionally, Hayam *et al.* conducted a survival analysis involving 259 elderly CRC patients (stage I–III) who underwent cancer-eradicating surgery, demonstrated that a preoperative GNRI below a defined cutoff was considerable tied to decreased OS (22). Our research demonstrate that $CD4^+$ T cells, double-positive T cells, double-negative T cells, B lymphocytes, NK cells, and the GNRI function as prognostic immunological biomarkers linked to enhanced OS in CRC patients. Conversely, elevated levels of $CD8^+$ T cells are tied to reduced OS, consistent with established findings in tumor immunology and clinical nutrition research.

Within the immune system, immune cells can directly or indirectly suppress oncogenesis and tumor progression through diverse immunological mechanisms. For example, $CD4^+$ T cells facilitate $CD8^+$ T cells activation and can mediate tumor cell lysis via expression of cytotoxic granules such as granzymes and perforin (23). B lymphocytes contribute to anti-neoplastic immunity by producing tumor-specific immunoglobulins (24). NK cells primarily combat tumors by releasing perforin and granzymes to cytotoxicity against tumor cells or by secreting cytokines such as INF-γ to

Table 3 LS-GNRI subgroup analysis

Patient characteristics	High LS-GNRI, n (%)	Mid LS-GNRI, n (%)	Low LS-GNRI, n (%)	P
Tumor location				0.002
Right colon	20 (14.8)	17 (40.5)	6 (25.0)	
Left colon and rectum	115 (85.2)	25 (59.5)	18 (75.0)	
Preoperative perforation/obstruction				0.06
Yes	7 (5.2)	6 (14.3)	4 (16.7)	
No	128 (94.8)	36 (85.7)	20 (83.3)	
Postoperative complications				0.43
Yes	9 (6.7)	5 (11.9)	1 (4.2)	
No	126 (93.3)	37 (88.1)	23 (95.8)	
CEA, ng/mL				0.002
≤5	101 (74.8)	24 (57.1)	10 (41.7)	
>5	34 (25.2)	18 (42.9)	14 (58.3)	
Tumor differentiation				0.008
Poor	20 (14.8)	5 (11.9)	8 (33.3)	
Moderate	99 (73.3)	37 (88.1)	16 (66.7)	
Well	16 (11.9)	0	0	
Tumor stage				0.18
I	30 (22.2)	7 (16.7)	1 (4.2)	
II	69 (51.1)	21 (50.0)	12 (50)	
III	36 (26.7)	14 (33.3)	11 (45.8)	
RAS				0.08
Mutant	48 (35.6)	23 (54.8)	10 (41.7)	
Wild-type	87 (64.4)	19 (45.2)	14 (58.3)	
BRAF				<0.001
Mutant	11 (8.1)	6 (14.3)	9 (37.5)	
Wild-type	124 (91.9)	36 (85.7)	15 (62.5)	
MSI				0.61
MSI-H	7 (5.2)	4 (9.5)	2 (8.3)	
MSS	128 (94.8)	38 (90.5)	22 (91.7)	
Adjuvant chemotherapy				0.03
Yes	81 (60.0)	27 (64.3)	21 (87.5)	
No	54 (40.0)	15 (35.7)	3 (12.5)	

CEA, carcinoembryonic antigen; LS-GNRI, lymphocyte subset-Geriatric Nutritional Risk Index; MSI, microsatellite-instability; MSI-H, microsatellite-instability high; MSS, microsatellite stable.

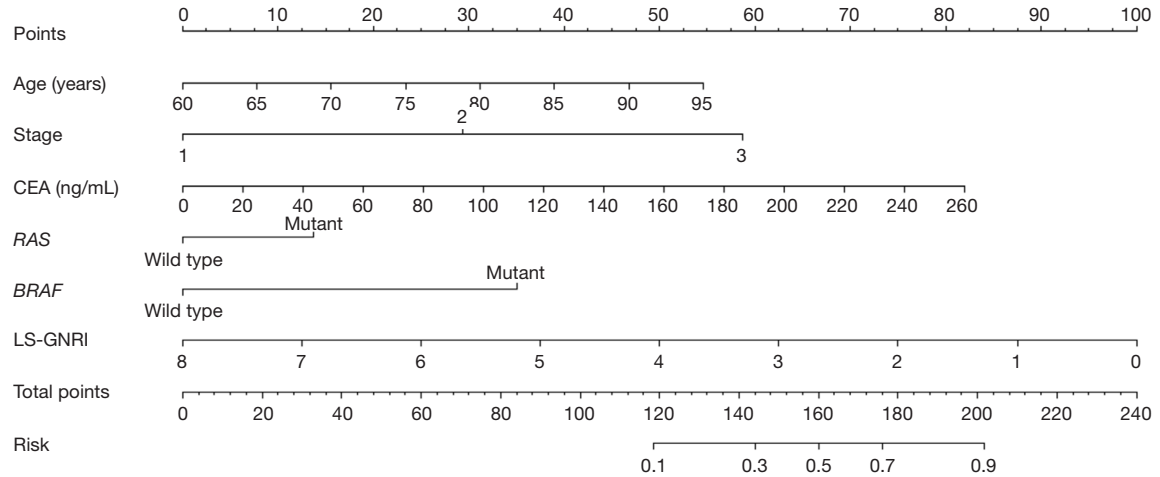

Figure 5 Nomogram composed of age, stage, CEA, and LS-GNRI. CEA, carcinoembryonic antigen; LS-GNRI, lymphocyte subset-Geriatric Nutritional Risk Index.

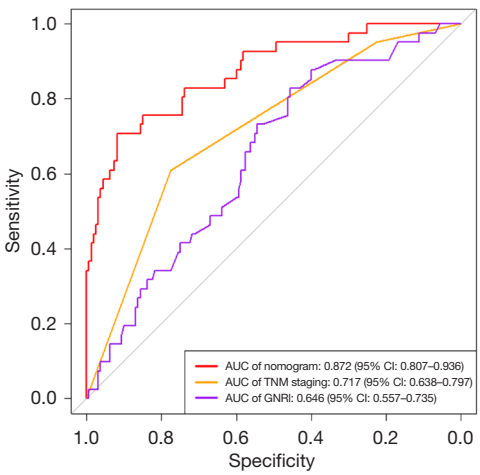

Figure 6 Comparison of AUC between three models. AUC, area under the curve; CI, confidence interval; GNRI, Geriatric Nutritional Risk Index; TNM, Tumor, Node, Metastasis.

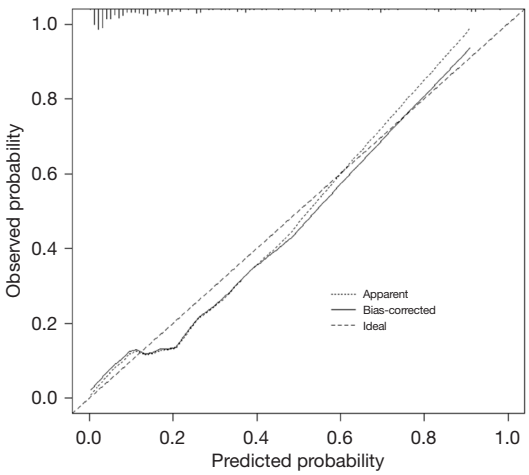

Figure 7 Evaluation of the fitting ability of the model, calibration curves.

regulate adaptive immune responses (25). In our investigation, we identified that the $CD8^+$ T cells to $CD4^+/CD8^+$ T cell ratio serves as a prognostic risk factors correlated with OS in geriatric CRC patients. An elevation in $CD8^+$ T lymphocyte counts indicates a state of immune hyperactivation accompanied by functional exhaustion, which correlates with unfavorable clinical prognoses. Current research indicates that $CD8^+$ T cell exhaustion and tumor-induced dysfunction of $CD8^+$ T cells are one of the critical immunopathological mechanisms contributing to oncogenesis. Persistent tumor antigen exposure drives differentiation of $CD8^+$ T cells into terminally exhausted phenotypes, marked by elevated expression of inhibitory receptors (PD-1, TIM-3, TIGIT) and anti-apoptotic molecules (e.g., Bcl-2). Despite compromised effector functions, these exhausted T cells persist as sustained residents within the peripheral circulation (26-28). An increased $CD4^+/CD8^+$ T cell ratio may reflect heightened $CD4^+$ T cells activation that potentially facilitates Th17 lineage differentiation, characterized by IL-17 secretion, which enhances tumor cell motility and proliferation (29). Simultaneously, a decline in $CD8^+$ cytotoxic T lymphocytes impairs effective

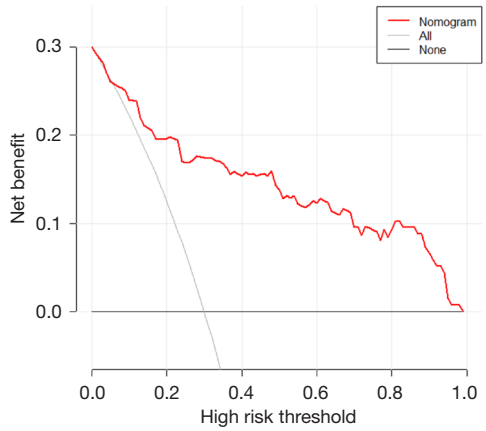

Figure 8 Evaluation of clinical decision-making ability of the model, DCA curve. DCA, decision curve analysis.

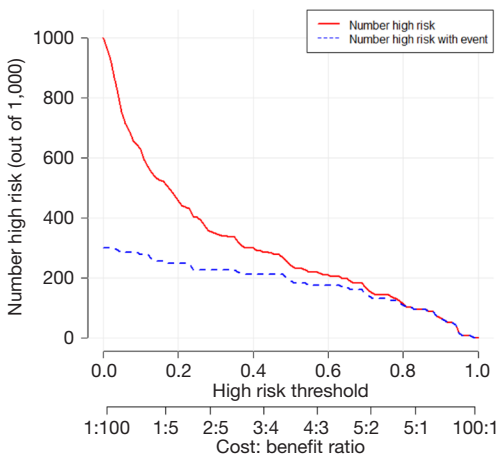

Figure 9 The clinical net benefits of the model under different risk thresholds, clinical impact curve.

antitumor immune responses. These observations imply that immune homeostasis operates through a finely tuned balance rather than simple immune augmentation. In guiding immunotherapeutic strategies for patients, it is essential to conduct individualized immunological assessments within clinical practice. An optimal immunomodulatory approach should aim to recalibrate the patient's immune equilibrium within a "therapeutic window" rather than simply enhancing or inhibiting immune responses. For example, novel approaches such as reversing immunosuppression and reversing T cell exhaustion can be employed. Additionally, investigating the effects of traditional treatments like surgery, radiotherapy, and chemotherapy on the dynamic changes of lymphocyte subpopulations will provide critical insights for optimizing therapeutic protocols.

Subsequently, this investigation utilized LASSO regression analysis to integrate lymphocyte subset profiles and GNRI, thereby constructing a novel composite hematological biomarker, LS-GNRI, which encapsulates the comprehensive immunonutritional status of oncological patients. Kaplan-Meier survival curves and Cox proportional hazards models revealed that elderly CRC patients with diminished LS-GNRI scores experienced considerable reduced OS and DFS. These results indicate that LS-GNRI is not only associated with prognostic stratification in elderly CRC populations but also functions as a standalone prognostic factor, underscoring its utility in predicting CRC outcomes. The pathophysiological mechanisms are primarily attributed to immunosenescence impairing anti-tumor immune surveillance, tumor-mediated immunosuppression, and malnutrition aggravating tumor aggressiveness. The deleterious feedback loop driven by immune decline and nutritional deficiency further accelerates mortality risk.

Following subgroup analysis of LS-GNRI, we identified that elevated and reduced LS-GNRI values are correlated with tumor laterality in elderly CRC patients: individuals with right-sided colon neoplasms demonstrate decreased LS-GNRI relative to those with left-sided lesions. This variation may be explained by multiple pathophysiological factors: in tumor tissues, right-sided colon cancers exhibit lower densities of $CD4^+$ T lymphocytes compared to left-sided counterparts, with functionally compromised $CD161^+$ $CD8^+$ T cells being enriched in right-sided tumors (30,31). The right colon's role in nutrient absorption—such as short-chain fatty acids and vitamin B12—implies that patients undergoing right hemicolectomy are at heightened risk for malnutrition. Furthermore, the tumor microenvironment in right-sided colon cancers often displays a more intense inflammatory response (32), which can facilitate muscle catabolism and metabolic dysregulation, thereby increasing vulnerability to nutritional deficiencies. Our research suggests that decreased LS-GNRI is associated with elevated CEA levels and poorer tumor differentiation, indicating that lower LS-GNRI may serve as a marker of increased tumor invasiveness. Firstly, regarding immunological determinants, immunosuppressive states can facilitate tumor invasiveness, while lymphocyte depletion, as an indicator of systemic immune suppression, compromises anti-tumor immune surveillance. For example, a decline in $CD4^+$ T cells—particularly within the Th1 subset—reduces activation of cytotoxic $CD8^+$ T lymphocytes and macrophages, thereby impairing their cytotoxic effector

functions. Additionally, region-specific $CD16^+$ neutrophil subsets may promote colorectal carcinogenesis through the suppression of NK cell cytotoxicity (33). The mechanisms responsible for elevated CEA levels in the context of immune suppression remain to be fully elucidated; however, it is postulated that tumor-associated inflammatory responses stimulate secretion of pro-inflammatory cytokines such as TNF-α and IL-6, which stimulate epithelial cells and macrophages to overexpress CEA, leading to increased circulating concentrations. Furthermore, poorly differentiated tumor tissues demonstrate increased infiltration of FoxP3+ regulatory T cells, which have been demonstrated to suppress effector immune responses and promote immune tolerance, potentially contributing to lymphocyte depletion. Concurrently, poor differentiation CRCs exhibit heightened infiltration of $CD163^+$ tumor-associated macrophages (TAM), with elevated $CD163^+$ TAM levels serving as adverse prognostic biomarkers (34,35). Our investigation further demonstrates that patients exhibiting lower LS-GNRI indices display a higher incidence of *BRAF* mutational status. This correlation seems to be linked with heightened pro-inflammatory cytokine expression and significant modulation of the tumor microenvironment's immune landscape. Notably, *BRAF* mutations are associated with increased inflammatory signaling pathways and a substantial influx of cytotoxic $CD8^+$ T lymphocytes within the tumor infiltrate (36). Elderly patients with CRC exhibit increased vulnerability to malnutrition relative to younger cohorts, primarily attributable to metabolic deterioration, compromised gastrointestinal absorption, and the influence of chronic comorbid conditions. Furthermore, age-associated atrophy of central lymphoid organs, coupled with declines in innate and adaptive immune responses, leads to immunosenescence (37,38). The concomitant deterioration of immune competence and nutritional deficiency synergistically facilitate tumorigenesis and disease progression through multiple pathophysiological pathways.

Overall, the LS-GNRI offers a comprehensive evaluation of patients' immunonutritional status, enabling precise prognostication of clinical outcomes in elderly CRC individuals. Additionally, the study examines the potential mechanistic role of LS-GNRI in CRC prognosis through its association with underlying biological pathways. However, several limitations should be acknowledged. First, the absence of external validation and the restricted participant pool could limit the applicability of our findings. Second, as a single-center retrospective analysis, the study is susceptible to potential selection bias. Future investigations should prioritize large-scale, multicenter prospective cohorts to corroborate our results. Furthermore, subsequent research could examine the possible synergistic benefits of combining nutritional interventions with immunomodulatory therapies in this high-risk population.

Conclusions

The LS-GNRI model and associated nomogram constructed in this investigation provide practical prognostic assessment instruments for geriatric CRC patients, thereby facilitating clinicians' decision-making processes concerning personalized therapeutic regimens and pharmacological interventions.

Acknowledgments

None.

Footnote

Reporting Checklist: The authors have completed the TRIPOD reporting checklist. Available at https://tcr.amegroups.com/article/view/10.21037/tcr-2025-1685/rc

Data Sharing Statement: Available at https://tcr.amegroups.com/article/view/10.21037/tcr-2025-1685/dss

Peer Review File: Available at https://tcr.amegroups.com/article/view/10.21037/tcr-2025-1685/prf

Funding: None.

Conflicts of Interest: All authors have completed the ICMJE uniform disclosure form (available at https://tcr.amegroups.com/article/view/10.21037/tcr-2025-1685/coif). The authors have no conflicts of interest to declare.

Ethical Statement: The authors are accountable for all aspects of the work in ensuring that questions related to the accuracy or integrity of any part of the work are appropriately investigated and resolved. The study was conducted in accordance with the Declaration of Helsinki and its subsequent amendments. The study was approved by the ethics committee of The First Affiliated Hospital of Chongqing Medical University (No. 2025-488-01) and individual consent for this retrospective analysis was waived.

References

1. Bray F, Laversanne M, Sung H, et al. Global cancer statistics 2022: GLOBOCAN estimates of incidence and mortality worldwide for 36 cancers in 185 countries. CA Cancer J Clin 2024;74:229-63.
2. Klimeck L, Heisser T, Hoffmeister M, et al. Colorectal cancer: A health and economic problem. Best Pract Res Clin Gastroenterol 2023;66:101839.
3. Bouvier AM, Jooste V, Lillini R, et al. Differences in survival and recurrence of colorectal cancer by stage across population-based European registries. Int J Cancer 2024;155:807-15.
4. Dekker E, Tanis PJ, Vleugels JLA, et al. Colorectal cancer. Lancet 2019;394:1467-80.
5. Gao S, Hsu TW, Li MO. Immunity beyond cancer cells: perspective from tumor tissue. Trends Cancer 2021;7:1010-9.
6. Lian J, Yue Y, Yu W, et al. Immunosenescence: a key player in cancer development. J Hematol Oncol 2020;13:151.
7. Zhang T, Wen R, Fan H, et al. Impact and potential value of immunosenescence on solid gastrointestinal tumors. Front Immunol 2024;15:1375730.
8. Li C, Jiang P, Wei S, et al. Regulatory T cells in tumor microenvironment: new mechanisms, potential therapeutic strategies and future prospects. Mol Cancer 2020;19:116.
9. Han S, Georgiev P, Ringel AE, et al. Age-associated remodeling of T cell immunity and metabolism. Cell Metab 2023;35:36-55.
10. Chapman NM, Chi H. Metabolic adaptation of lymphocytes in immunity and disease. Immunity 2022;55:14-30.
11. Lin B, Du L, Li H, et al. Tumor-infiltrating lymphocytes: Warriors fight against tumors powerfully. Biomed Pharmacother 2020;132:110873.
12. Zhou J, Lin HP, Xu X, et al. The predictive value of peripheral blood cells and lymphocyte subsets in oesophageal squamous cell cancer patients with neoadjuvant chemoradiotherapy. Front Immunol 2022;13:1041126.
13. Xia Y, Li W, Li Y, et al. The clinical value of the changes of peripheral lymphocyte subsets absolute counts in patients with non-small cell lung cancer. Transl Oncol 2020;13:100849.
14. Okamura K, Wang L, Nagayama S, et al. Characterization of double-negative T cells in colorectal cancers and their corresponding lymph nodes. Oncoimmunology 2024;13:2373530.
15. Salas S, Cottet V, Dossus L, et al. Nutritional Factors during and after Cancer: Impacts on Survival and Quality of Life. Nutrients 2022;14:2958.
16. Martínez-Escribano C, Arteaga Moreno F, Pérez-López M, et al. Malnutrition and Increased Risk of Adverse Outcomes in Elderly Patients Undergoing Elective Colorectal Cancer Surgery: A Case-Control Study Nested in a Cohort. Nutrients 2022;14:207.
17. Dent E, Wright ORL, Woo J, et al. Malnutrition in older adults. Lancet 2023;401:951-66.
18. Bouillanne O, Morineau G, Dupont C, et al. Geriatric Nutritional Risk Index: a new index for evaluating at-risk elderly medical patients. Am J Clin Nutr 2005;82:777-83.
19. Yuan C, Huang J, Li H, et al. Association of clinical outcomes and the predictive value of T lymphocyte subsets within colorectal cancer patients. Front Surg 2023;10:1102545.
20. Gao C, Tong YX, Zhu L, et al. Short-term prognostic role of peripheral lymphocyte subsets in patients with gastric cancer. Int Immunopharmacol 2023;115:109641.
21. Mao F, Yang C, Luo W, et al. Peripheral blood lymphocyte subsets are associated with the clinical outcomes of prostate cancer patients. Int Immunopharmacol 2022;113:109287.
22. Hayama T, Hashiguchi Y, Ozawa T, et al. The preoperative geriatric nutritional risk index (GNRI) is an independent prognostic factor in elderly patients underwent curative resection for colorectal cancer. Sci Rep 2022;12:3682.
23. Oh DY, Fong L. Cytotoxic CD4(+) T cells in cancer: Expanding the immune effector toolbox. Immunity 2021;54:2701-11.
24. Laumont CM, Nelson BH. B cells in the tumor microenvironment: Multi-faceted organizers, regulators, and effectors of anti-tumor immunity. Cancer Cell 2023;41:466-89.
25. Wu SY, Fu T, Jiang YZ, et al. Natural killer cells in cancer biology and therapy. Mol Cancer 2020;19:120.
26. Ding JT, Yang KP, Zhou HN, et al. Landscapes and mechanisms of CD8(+) T cell exhaustion in gastrointestinal cancer. Front Immunol 2023;14:1149622.

27. Zhong T, Sun S, Zhao M, et al. The mechanisms and clinical significance of CD8(+) T cell exhaustion in anti-tumor immunity. Cancer Biol Med 2025;22:460-80.
28. Philip M, Schietinger A. CD8(+) T cell differentiation and dysfunction in cancer. Nat Rev Immunol 2022;22:209-23.
29. Pan Y, Yang W, Tang B, et al. The protective and pathogenic role of Th17 cell plasticity and function in the tumor microenvironment. Front Immunol 2023;14:1192303.
30. Liu B, Li S, Cheng Y, et al. Distinctive multicellular immunosuppressive hubs confer different intervention strategies for left- and right-sided colon cancers. Cell Rep Med 2024;5:101589.
31. Hu Y, Ding J, Wu C, et al. Differential Expression and Prognostic Correlation of Immune Related Factors Between Right and Left Side Colorectal Cancer. Front Oncol 2022;12:845765.
32. Patel M, McSorley ST, Park JH, et al. The relationship between right-sided tumour location, tumour microenvironment, systemic inflammation, adjuvant therapy and survival in patients undergoing surgery for colon and rectal cancer. Br J Cancer 2018;118:705-12.
33. Zhang Y, Wang Z, Lu Y, et al. Region-Specific CD16(+) Neutrophils Promote Colorectal Cancer Progression by Inhibiting Natural Killer Cells. Adv Sci (Weinh) 2024;11:e2403414.
34. Wang X, Bai Y, Zhou Z, et al. Relationship Between Infiltration of CD163+ TAMs, FoxP3+ Tregs, or CD66b+ TANs and Cell Differentiation in Colorectal Cancer Tissues. Turk J Gastroenterol 2023;34:747-52.
35. Xue T, Yan K, Cai Y, et al. Prognostic significance of CD163+ tumor-associated macrophages in colorectal cancer. World J Surg Oncol 2021;19:186.
36. Salem ME, Puccini A, Mauer E, et al. Impact of RAS/BRAF V600E mutations on the tumor immune microenvironment in mismatch repair deficient / microsatellite instability colorectal cancers. Clin Cancer Res 2026;32:417-27.
37. Weiskopf D, Weinberger B, Grubeck-Loebenstein B. The aging of the immune system. Transpl Int 2009;22:1041-50.
38. Feehan J, Tripodi N, Apostolopoulos V. The twilight of the immune system: The impact of immunosenescence in aging. Maturitas 2021;147:7-13.

Cite this article as: Wang Y, Hao Y, Jia H. Preoperative peripheral blood lymphocyte subsets integrated with geriatric nutritional risk index for prognostic assessment in elderly colorectal carcinoma patients. Transl Cancer Res 2026;15(1):22. doi: 10.21037/tcr-2025-1685